Liuyang Bai*

Preparation and characterization of Ni-Cu composite nanoparticles for conductive paints

https://doi.org/10.1515/secm-2019-0011
Received March 13, 2019; accepted Aprl 16, 2019

Abstract: Ni and Cu are the two most promising alternatives to noble metals used in electrical conductive materials. However, Cu is susceptible to oxidation, while Ni exhibits poorer electrical conductivity. To solve this problem, Cu-Ni composite nanoparticles have been prepared in the present work by successive hydrazine reduction based on the different oxidation potential between Cu (II) and Ni (II). The as-prepared products were characterized by XRD, FE-SEM, EDS, and TG, and the electrical resistivity of which was measured by four-probe method. A formation process of the composite particles was proposed and demonstrated. The Cu-Ni composite nanoparticles have a uniform diameter of about 50nm, and exhibit higher oxidation temperature than Cu and lower electrical resistivity than Ni. This novel Ni-Cu structure and method might help solve the problems associated with the oxidation of Cu and the low electrical conductivity of Ni, which would further promote the application of base metal conductive powders.

Keywords: metallic powders, composite nanoparticles, electrical conductivity, oxidation resistance

1 Introduction

Composite particles combining two or more components in each individual particle usually exhibit novel or multiple properties and hence have much broader applications than their homogeneous single-component counterparts [1–4]. Therefore, new synthesis strategies to prepare composite powders have attracted considerably increasing attention in recent years, particularly if they are straightforward to implement and can be applied to potentially useful materials [5, 6].

Metal powders with high conductivity, such as Au, Pd, Ag, Cu, Ni, Co, and Al, are used as the conductive fillers, which are applied to printed circuitboards, display touch panel electrodes, electromagnetic interference (EMI) shielding, solar cell, and silicone rubber [7–10]. Conventionally, conductive materials and components are usually made from noble metals such as Ag and Pd due to their good electrical conductivity and high resistance to oxidation. However, the increasingly high cost has considerably limited its practical and industrial applications. In recent years, base metals such as Ni and Cu are seen as more economical alternatives to noble metals and are extensively investigated[11-15]. Cu exhibits good electrical conductivity as high as that of Ag, but susceptible to oxidation. To solve this problem, different approaches have been explored to protect Cu from oxidation [16–18]. Compared to Cu, Ni exhibits better oxidation resistance and poorer conductivity. In order to overcome the problems associated with the oxidation of Cu and the low electrical conductivity of Ni, Ni-coated Cu particles have been explored [19–22]. Kim report a highly effective strategy to improve the chemical resistance of a Cu particulate film-based electrode by coating a Ni protective shell on the surface of the Cu nanoparticles without degrading their electrical conductivity, and the electrical conductivity and resistance to oxidation of the Cu@Ni electrodes could be precisely controlled by adjusting the thickness of the Ni shell [11]. In a typical coating technique, the core particles are usually synthesized ahead, and then added into the plating solution for coating [23]. It is known that passivation is always necessary for the synthesis of Cu nanoparticles because fine Cu particle readily oxidizes in air [24, 25]. Therefore, surface treatment of Cu particles must be carried out to remove the passive coat before Ni plating, which would make the coating process complicated. There is also some one-step method proposed. For example, Mancier washed and dried the fresh copper powders under vacuum, and then immediately introduced them into silver solution for coating [26]. However, it was still impossible to eliminate the oxygen contamination completely during this process.

In the present work, a facile successive reduction route to antioxidant Ni-Cu composite nanoparticles was designed and demonstrated. The difference of oxidation

***Corresponding Author: Liuyang Bai:** Zhumadian Academy of Industry Innovation and Development, Huanghuai University, Zhumadian, 463000, P. R. China; E-mail lybai@huanghuai.edu.cn
State Key Laboratory of Multi-phase Complex Systems, Institute of Process Engineering, Chinese Academy of Sciences, Beijing 100190, P. R. China; E-mail lybai@ipe.ac.cn

Open Access. © 2019 Liuyang Bai, published by De Gruyter. This work is licensed under the Creative Commons Attribution alone 4.0 License

potential between Cu (II) and Ni (II) was exploited and the reduction process was designed and controlled. With Cu and Ni salts coexisting in the hydrazine reduction system, Cu (II) was firstly reduced and acted as the nuclei, and Ni (II) was reduced afterwards and directly coated on the Cu particles. No protecting agents or surface treatments were needed. The objective of this work is to create low-cost electrical conductive particles that can overcome the problems brought by the oxidation of Cu and low electrical conductivity of Ni.

2 Materials and Methods

All analytical chemical reagents were obtained from Beijing Chemical Reagents Co. and used without further purification. Typically, an appropriate amount of $NiCl_2{\cdot}6H_2O$ and $CuSO_4{\cdot}5H_2O$ were dissolved into 100 mL of distilled water to get homogeneous aqueous solution with a total concentration of 0.1M. The molar ratio of $NiCl_2{\cdot}6H_2O/CuSO_4{\cdot}5H_2O$ was controlled at 1:0, 2:1; 1:1, 1:2, and 0:2 for Ni, Ni2Cu1, Ni1Cu1, Ni1Cu2, and Cu, respectively. The solution was heated in thermostatic water bath till the temperature reached 80°. Then 2.5 mL of $N_2H_4{\cdot}H_2O$ (85 wt.%) was injected into the solution. The mixture was stirred and heated for another 1h. After cooled to room temperature naturally, the precipitates were filtered off and washed with distilled water and anhydrous ethanol in sequence and then dried at 60° for 1 h. $NH_3{\cdot}H_2O$ can be used for adjusting pH value if one wants to reduce the amount of $N_2H_4{\cdot}H_2O$. In order to obtained pure Ni powders, the amount of $N_2H_4{\cdot}H_2O$ was kept at 1.7 mL, and NaOH was supplied with the molar ratio of OH^-/Ni^{2+} at 3.

The crystalline phase of the as-prepared samples was characterized by X-ray diffractometry (XRD, X'pert PRO, Panalytical, CuKα radiation) in a 2θ range from 10° to 90°. Their size and morphology were inspected with field scanning electron microscopy (FE-SEM, JEOL JSM- 6700F). Energy dispersive spectroscope (EDS) coupled with FE-SEM was used to investigate the chemical composition and topography. The thermal stability of the products was recorded using a thermal analyzer (Netzsch STA 449 TG-DTA/DSC) in air with the heating rate of 10°/min up to 900°.

The electrical resistivity of which was measured by a straight-line vertical four-probe method at room temperature. The constant current was supplied through a Hall measuring controller and the voltage was measured by a nanovolt meter, as shown in Figure 1. Similar experimental setups were commonly used in the literature [27, 28].

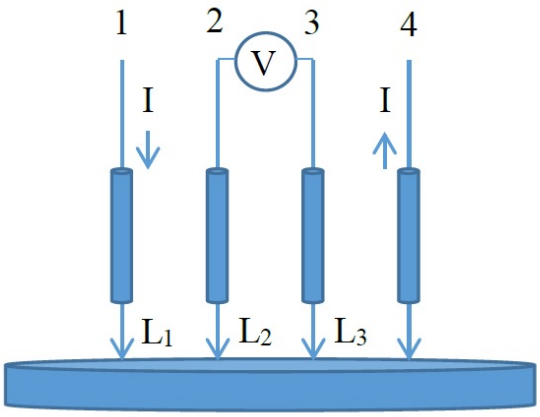

Figure 1: Four-probe scheme for electrical resistivity measurement, redrawn according to Ref. [28].

The current flowing through probes 1 and 4 is I, and the measuring voltage between probes 2 and 3 is V. The distances between probes are L_1, L_2 and L_3, respectively. The conductivity of the electrode can be calculated by the following Eq. (1), where $L_1 = L_2 = L_3 = L = 1$ mm, so the Eq. (1) can be simplified and the resistivity can be to calculated by Eq. (2).

$$\sigma = \frac{I}{2\pi V}\left(\frac{1}{L_1} - \frac{1}{L_3} - \frac{1}{L_1 + L_2} + \frac{1}{L_2 + L_3}\right) \quad (1)$$

$$\rho = \frac{1}{\sigma} = \frac{2\pi VL}{I} \quad (2)$$

3 Results and discussion

3.1 Reduction process

Hydrazine (N_2H_4) is a powerful cheap reductant widely used for the production of fine metallic powders. The hydrazine reduction process can be given as Eq. (3).

$$2M^{2+} + N_2H_4 + 4OH^- \rightarrow 2M(s) + N_2(g) + 4H_2O \quad (3)$$

The reducing capability of N_2H_4 is highly dependent on the reaction temperature and pH value of the solution. In the present experiment, the alkalinity condition provided by $N_2H_4{\cdot}H_2O$ or $NH_3{\cdot}H_2O$ was weak and the reaction temperature was controlled below 80°. Cu (II) can be reduced under such mild condition while Ni (II) can not, for Ni (II) has lower oxidation potential than Cu (II). However, Ni (II) was reduced in our experiments as long as solid additives such as Ag powders, fresh Cu powders, or Si powders were added into the reduction system. The powders

after Ni plating exhibited magnetic properties and could all be collected with a magnet. It's known that Cu and Si have no catalytic effect on hydrazine reduction of Ni (II), so the solid additives must have played the role of nucleating agents [29].

Inspired by these experimental results, we proposed the facile successive hydrazine reduction route to Cu-Ni composite particles. Figure 2 illustrates an ideal formation process of the composite particles.

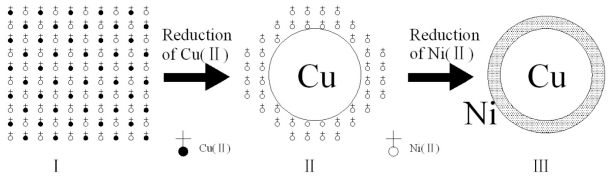

Figure 2: Illustration of the ideal formation process of the Cu-Ni composite particles: step , Cu (II) and Ni (II) co-existence; step , reduction of Cu (II); step III, reduction of Ni (II).

When Cu (II) and Ni (II) co-exist in the hydrazine reduction system (step in scheme 1), Cu (II) would be reduced first and form Cu particles (step II in scheme 1), and then, the newly-formed Cu particles act as nucleus and trigger the reduction of Ni (II) (step III in scheme 1). Because Ni (II) is stable in the present deposition system without Cu, no homogeneous nucleation could be observed when the Ni plating solution was heated for 1 h. Therefore, it is reasonable that the former formed Cu nucleus played the role of nucleating agent and the later reduced Ni deposited on the surface and formed Ni-coated Cu composite particles.

In order to demonstrate the reaction system more clearly, macroscopical Si foil or activated carbon fibers instead of Cu (II) were added into the mild Ni plating solution. Upon the addition of a cleaned Si foil into the plating bath composed of $NH_3 \cdot H_2O$ and $N_2H_4 \cdot H_2O$, there existed bubbles arising from its surface, indicating that the hydrazine reduction process had been triggered by the Si foil. On one hand, the Si foil after Ni-plating kept smooth but exhibited magnetic properties, indicating that Ni had been uniformly plated on the surface of Si foil. On the other hand, no isolated Ni particles could be collected by magnet from the used plating solution, indicating that Ni particles had not formed by way of homogeneous nucleation.

Figure 3a and b are photos of Si foil before and after Ni-plating, respectively. The Si foil after coating by nickel looked smooth as before but the color turned dark. Figure 3c is a picture showing the magnetism properties of Ni-coated Si foil intuitively. Figure 3d is the SEM image of the coated Si foil surface and Figure 3e is the corresponding EDS results. It can be seen clearly that Ni particles (confirmed by the EDS results) deposited on the surface. The morphology of Ni particles is in consistent with that deposited on activated carbon fibers and pure Ni powders.

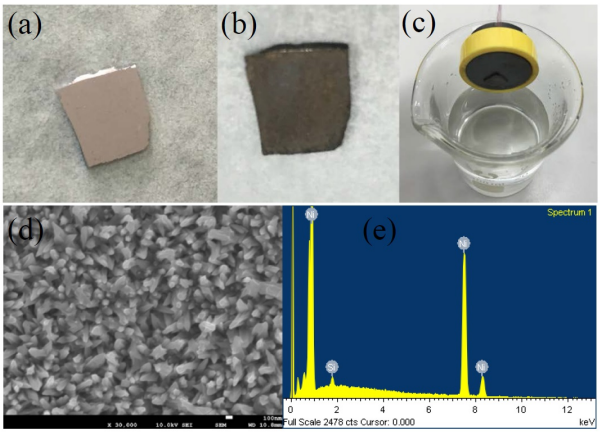

Figure 3: Photos of Si foil before Ni-plating (a), after Ni-plating (b), absorbed by a magnet after Ni-plating, and SEM image (d) of Ni-coated Si foil surface and the corresponding EDS result (e).

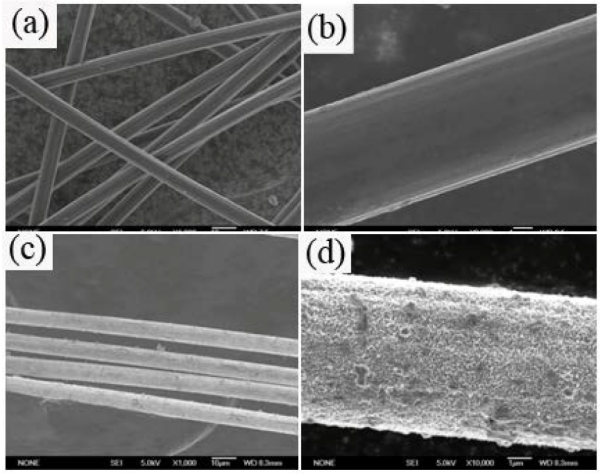

Figure 4: FESEM of the carbon fibers before (a-b) and after(c-d) coated by nickel.

Similar phenomena occurred when activated carbon fibers were used instead of Si foil. The carbon fibers after coated exhibited magnetic properties and can all be absorbed by a magnet. Figure 4 shows FESEM of the carbon fibers before (a-b) and after (c-d) Ni-coated. It can be seen that surface of carbon fibers before Ni-coated are very smooth, which changes obviously after Ni-coated. The Ni

coating on the surface of carbon fibers is compact and tight. No isolated Ni particles can be observed between the fibers under FESEM observation. Therefore, it can be concluded that the proposed Ni plating solution is stable enough that the formation of isolated Ni particles can be eliminated.

It was also demonstrated in our preliminary experiments that the reduction of Ni (II) had an induction time as long as 10 min even when the reaction temperature was raised above 120°, while the reduction of Cu (II) occurred immediately upon the injection of $N_2H_4 \cdot H_2O$ and completed within several minutes at the temperature of 80° [30]. Therefore, the reduction process of Cu (II) and Ni (II) can be divided clearly into two steps: reduction of Cu (II) and reduction of Ni (II). The difference in the reaction time contributed to the formation of coated structures rather than Ni-Cu alloys. The successive reduction process can also be observed during the experiments. With the addition of $N_2H_4 \cdot H_2O$, the solution turned red immediately, indicating that Cu (II) was reduced and metallic Cu particles formed. With the reaction time prolonged to more than 10 minutes, the solution turned gray and then black, which is the color of Ni, indicating that the surface of Cu particles was covered by Ni.

3.2 Characteristics of the products

Figure 5 shows XRD patterns of the products obtained with the molar ratio of Ni/Cu at 1:0, 2:1, 1:1, 1:2, and 0:2 respectively. All diffraction peaks were attributed to Cu and Ni, indicating that not only Cu but also Ni can be obtained in the present system. With the increase of the molar ratio of Ni/Cu, the diffraction peaks of Ni was significantly enhanced. When a ratio Ni/Cu = 1 is used, the peaks of Cu and Ni can not separate clearly from each other and exist as almost one. However, it can still recognized in the High-score software as Ni and Cu respectively. On the other hand, the main peaks of Ni1Cu1 is perfectly agree with that of Cu instead of between Cu and Ni. Therefore, overlap of the peaks attributes to the little distance between them instead of formation of alloys.

Figure 6a shows the FESEM image of products obtained with the molar ratio of Ni/Cu at 1. The sample is composed of well-dispersed spheres, the average diameter of which is about 50 nm. Figure 6b shows the FESEM image of the Cu powders obtained under similar experimental conditions when $CuSO_4 \cdot 5H_2O$ was used only. Figure 6c shows the FESEM image of the Ni powders obtained under similar experimental conditions when the amount of $N_2H_4 \cdot H_2O$ was kept at 1.7 mL, and NaOH was supplied

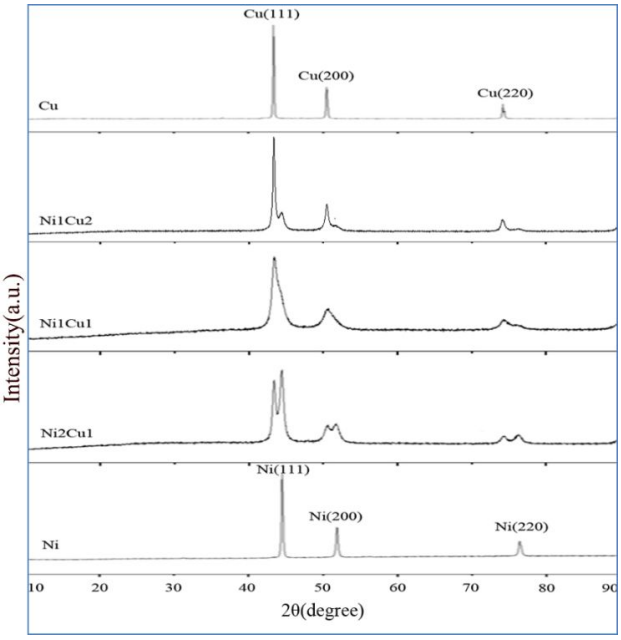

Figure 5: XRD patterns of Ni, Ni2Cu1, Ni1Cu1, Ni1Cu2, Cu nanoparticles.

with the molar ratio of OH^-/Ni^{2+} at 3. It can be seen that Cu-Ni composite particles have similar shape and size with the Cu particles, while Ni particles are flowerlike clusters. However, there are no Ni clusters detected in the Cu-Ni composite powders. These results further confirmed that the formation process of the Cu-Ni composite particles. It was reported that the oxidation resistance of Cu particles could also be greatly improved even when the particle surface was dotted by oxidation-resistant materials, because the active spot on the surface of Cu particles would be covered first [31]. So further study was directly conducted on the oxidation resistance instead of focus on the completeness of the Cu-Ni core-shell structure.

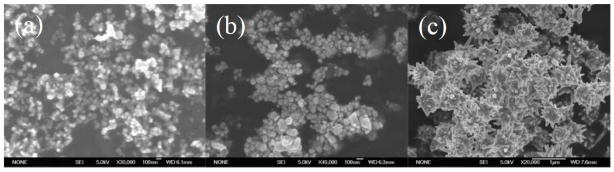

Figure 6: FESEM images of Ni, Cu, and Ni1Cu1 nanoparticles.

Figure 7 shows the EDS results of the sample with the Ni/Cu value of 2.0. Figure 7a and b is the Cu and Ni elemental map analysis, respectively. It can be seen that the distribution of Cu and Ni elements are homogeneous. The results according to Figure 7c showed 66.12wt.% and 33.88wt.% of Ni and Cu, respectively, and the molar ratio of

Ni/Cu is 2.1, which is appropriately in consistent with the theoretically calculated results according to the amount of raw material added. Because of the core-shell structure of the particles, copper is covered by nickel, which may be the reason why the detection rate of nickel/copper is slightly higher than the calculated value. The EDS results demonstrate the total element ratio of Ni/Cu, which is in agreement with the specific synthesis parameters.

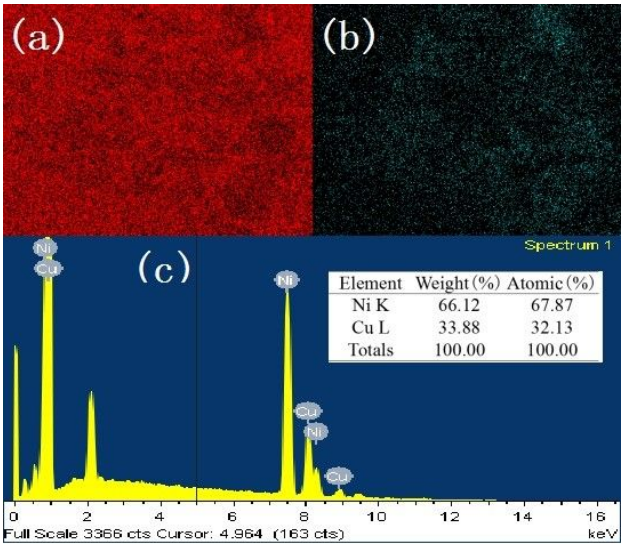

Figure 7: EDS results of the sample with the Ni/Cu value of 2.0.

The oxidation resistance of the sample in atmosphere was examined by TG. Figure 8 shows TG curves of the pure Cu powders (a) and the Ni-coated Cu composite powders (b) obtained with the molar ratio of Ni/Cu at 1. The obvious weight gain of Cu powders occurs at about 150° and the obvious weight gain of the composite powders occurs at about 270°, indicating the oxidation temperature of the two samples were about 150° and 270°, respectively. The oxidation temperature of the Ni-coated Cu composite powders is similar to that of pure Ni nanoparticles [32]. Therefore, the oxidation resistance of Cu powders was improved greatly after coated by Ni. The TG examination also showed indirectly that the obtained sample was the Ni-coated Cu composite instead of the mixture of Ni and Cu powders.

In order to examine the electrical conductivity, powders were treated at 200° in the mixture of H_2 (5%) and N_2 (95%) flow according to the literature [33], aiming to remove the contamination on their surface. Ultrafine Cu powders are readily to oxidized and turned to black from red during the filtration and drying. Treatment would provide the Ni-Cu and Cu powders in similar conditions when

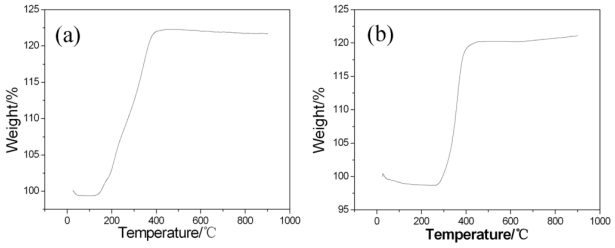

Figure 8: TG curves of Cu (a) and Ni-coated Cu (b) powders.

they were used and the conductivity were compared. Then post-treated powders were pressed into coin shape under the pressure of 100 kg. Photos of the samples for electrical conductivity measurements are shown in Figure 9.

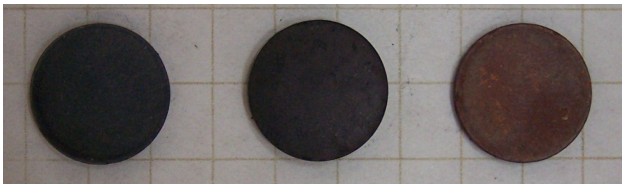

Figure 9: Photos of the samples for electrical conductivity measurements.

The resistivity was measured by four-probe method and the calculated results are given in Table 1. The resistivity of Cu powders, Ni powders, Ni1Cu1, and Ni1Cu2 composite powders were $1.8*10^{-6}\Omega\cdot m$, $9.1*10^{-6}\Omega\cdot m$, $6.2*10^{-6}\Omega\cdot m$, and $4.7*10^{-6}\Omega\cdot m$ respectively. Cu powders have expected lowest resistivity. In addition, the Ni-coated Cu composite powders exhibits lower electrical resistivity than Ni powders under similar condition.

4 Conclusions

A novel Ni-Cu structure was designed and the composite powders were prepared by successive hydrazine reduction. The powders were composed of well-dispersed nanoparticles and the particle size is about 50 nm. The distribution of Cu and Ni phases are homogeneous within the powders. The composite powders exhibit higher oxidation temperature than Cu and lower electrical resistivity than Ni. The innovative product might have potential application as conductive particles. This work might help solve the problems associated with the oxidation of Cu and the low electrical conductivity of Ni, which would further promote the application of base metal conductive powders.

Table 1: Conductivity of Cu, Ni, Ni1Cu1, and Ni1Cu2 powders.

Sample	Cu	Ni	Ni1Cu1	Ni1Cu2
Resistivity/Ω·m	$1.8*10^{-6}$	$9.1*10^{-6}$	$6.2*10^{-6}$	$4.7*10^{-6}$

Funding: This work was financially supported by the National Natural Science Foundation of China (No. 11875284).

References

[1] N. Farahbakhsh, S. Sanjabi, J. Ind. Eng. Chem. 2019, 70, 211.
[2] R. O. Apaydın, B. Ebin, S. Gürmen, Metall Mater. Trans A. 2016, 47, 3744.
[3] W. J. Lee, Y. K. Park, J. S. Kim, B. J. Kim, K. H. An, H. Lee, S. C. Jung, J. Nanosci. Nanotechnol. 2019, 19, 2362.
[4] X. F. Hou, Y. H. Zhang, H. Ding, P. K. Chu, Particuology 2018, 40, 105.
[5] K. J. Carroll, S. Calvin, T. F. Ekiert, K. M. Unruh, E. E. Carpenter, Chem. Mater. 2010, 22, 2175.
[6] P. Majerič, D. Jenko, B. Friedrich, R. Rudolf, Metals 2018, 8, 278
[7] Y. S. Park, C. Y. An, P. K. Kannan, N. Seo, K Zhuo, T. K. Yoo, C. H. Chung, Appl. Surf. Sci. 2016, 389, 865.
[8] Q. Dong, C. Huang, G. J. Duan, F. Zhang, D. A. Yan, Mater. Lett. 2017, 186, 263.
[9] E. B. Choi, J. H. Lee, Appl. Surf. Sci. 2017, 415, 67.
[10] L. Avramović, V. M. Maksimović, Z. Baščarević, N. Ignjatović, M. Bugarin, R. Marković, N. D. Nikolić, Metals 2019, 9, 56.
[11] T. G. Kim, H. J. Park, K. Woo, S. Jeong, Y. Choi, S. Y. Lee, ACS Appl. Mater. Interfaces 2018, 10, 1059.
[12] B. Madavali, J. H. Lee, J. K. Lee, K. Y. Cho, S. Challapalli, S. J. Hong, Powder Technol. 2014, 256, 251.
[13] L. Y. Bai, H. B. Zhang, H. C. Jin, J. cluster Sci. 2012, 23, 357.
[14] S. Mahadevan, A. P. S. Chauhan, Adv. Powder Technol. 2016, 27, 1852.
[15] K. Aruna, K. Aravindha, S. Karthikeyanb, P. A. Jeeva, K. Raja, Mater. Today: Proceedings 2018, 5, 13102.
[16] X. G. Cao, H. Y. Zhang, Powder Technol. 2012, 226, 53.
[17] W. L. Li, H. Zhang, Y. Gao, J. T. Jiu, C. F. Li, C. T. Chen, D. W. Hu, Y. Goya, Y. T. Wang, H. Koga, S. Nagao, K. Suganuma, J. Mater. Chem. C 2017, 5, 1155.
[18] G. Kawamura, S. Alvarez, I. E. Stewart, M. Catenacci, Z. F. Chen, Y. C. Ha, Sci. Rep. 2015, 5, 18333.
[19] Y. G. Guo, L. J. Wan, J. R. Gong, C. L. Bai, Phys. Chem. Chem. Phys. 2002, 4, 3422.
[20] M. A. Willard, L. K. Kurihara, E. E. Carpenter, S. Calvin, V. G. Harris, Int. Mater. Rev. 2004, 49, 125.
[21] J. Chen, J. Chen, Y. Li, W. X. Zhou, X. M. Feng, Q. L. Huang, J. G. Zheng, R. Q. Liu, Y. W. Ma, W. Huang, Nanoscale 2015, 7, 16874.
[22] T. Sakaue, K. Furumoto, K. Yoshimaru, JP. 013122, 2005.
[23] R. Xu, K. G. Zhou, M. Y. Hu, Rare Metal Mater. Eng. 2008, 37, 905.
[24] S. J. Oh, Y. Jo, E. J. Lee, S. S. Lee, Y. H. Kang, H. J. Jeon, S. Y. Cho, J. S. Park, Y. H. Seo, B. H. Ryu, Y. Choi, S. Jeong, Nanoscale 2015, 7, 3997.
[25] B. K. Park, S. Jeong, D. Kim, J. Moon, S. Lim, J. S. Kim, J. Colloid. Interface Sci. 2007, 311, 417.
[26] V. Mancier, C. Rousse-Bertrand, J. Dille, J. Michel, P. Fricoteaux, Ultrason. Sonochem. 2010, 17, 690.
[27] S. Pérez-Rodríguez, D. Torres, M. J. Lázaro, Powder Technol. 2018, 340, 380.
[28] J. M. Montes, F. G. Cuevas, J. Cintas, J. M. Gallardo, J. Mater. Sci. 2016, 51, 822.
[29] X. X. Jiang W. Shen, The Fundamentals and Practice of Electroless Plating, National Defense Industry Press, Beijing, China, 2000.
[30] L. Y. Bai, F. L. Yuan, Q. Tang, J. L. Li, H. Ryu, J. Mater. Sci. 2008, 43, 1769.
[31] B. J. Gao, J. F. Gao, H. M. Jiang, Z. X. Zhang, Acta Phys.-Chim. Sin. 2000, 16, 366.
[32] L. Y. Bai, J. M. Fan, P. Hu, F. L. Yuan, J. L. Li, Q. Tang, J Alloys Compd. 2009, 48, 1563.
[33] K. Bangshang, K. Qitai, J. Keyan. Manufacturing methods of nickel-plated copper powder and nickel-plated copper powder. China Patent, 200580024434.4